NUCLEAR PHYSICS A

Chiral pion–nucleon dynamics in finite nuclei: Spin–isospin excitations

P. Finelli [a,b,*], N. Kaiser [b], D. Vretenar [c], W. Weise [b]

[a] *Physics Department, University of Bologna, Italy*
[b] *Physik-Department, Technische Universität München, Germany*
[c] *Physics Department, Faculty of Science, University of Zagreb, Croatia*

Abstract

The nuclear density functional framework, based on chiral dynamics and the symmetry breaking pattern of low-energy QCD, is extended to the description of collective nuclear excitations. Starting from the relativistic point-coupling Lagrangian introduced in [P. Finelli, N. Kaiser, D. Vretenar, W. Weise, Nucl. Phys. A 770 (2006) 1], the proton–neutron (quasiparticle) random phase approximation is formulated and applied to investigate the role of chiral pion–nucleon dynamics in excitation modes involving spin and isospin degrees of freedom, e.g. isobaric analog states and Gamow–Teller resonances.
© 2007 Elsevier B.V. All rights reserved.

PACS: 21.30.Fe; 21.60.Jz; 24.30.Cz

1. Introduction

In a series of recent articles [1–6] we have developed a novel approach to nuclear density functional theory which emphasizes the relationship between aspects of low-energy, non-perturbative QCD and the nuclear many-body dynamics. A relativistic nuclear energy density functional has been formulated, starting from two basic features which establish the link with low-energy QCD and its symmetry-breaking pattern: (a) strong scalar and vector fields related to in-medium changes of QCD vacuum condensates; (b) long- and intermediate-range interactions generated

* Corresponding author at: Physics Department, University of Bologna, Italy.
 E-mail address: paolo.finelli@bo.infn.it (P. Finelli).

by one-and two-pion exchange, derived from in-medium chiral perturbation theory, with explicit inclusion of $\Delta(1232)$ excitations and in combination with three-nucleon (3N) interactions.

The resulting nuclear matter energy density functional [6] is mapped [3] onto the exchange-correlation energy density functional of a covariant point-coupling model for finite nuclei, including second order gradient corrections. In this approach the nuclear ground state is determined by the self-consistent solution of the relativistic generalizations of the linear single-nucleon Kohn–Sham equations. The construction of the density functional involves an expansion of nucleon self-energies in powers of the Fermi momentum up to and including terms of order k_f^6. In comparison with purely phenomenological mean-field models, the built-in QCD constraints and the explicit treatment of pion exchange restrict the freedom in adjusting parameters and functional forms of the density-dependent couplings. This approach to nuclear dynamics has been tested in an analysis of ground-state properties of a broad range of spherical and deformed nuclei [1]. The results have been compared with experimental data on binding energies, charge radii, neutron radii and deformation parameters for several isotopic chains. It has been demonstrated that the results for nuclear ground-state properties are at the same level of quantitative comparison with data as the best phenomenological relativistic mean-field models.

In this work the low-energy QCD-constrained nuclear density functional framework will be extended to the description of excited states and, in particular, to spin–isospin collective excitations. Starting from the relativistic point-coupling Hartree–Bogoliubov model of Ref. [1], we formulate the proton–neutron (quasiparticle) random phase approximation (PN-QRPA). This is then applied in an analysis of isobaric analog states and Gamow–Teller resonances in doubly-closed and open-shell nuclei. Our aim is to study the role of chiral pion–nucleon dynamics in charge-exchange modes. The results will be compared with available data, and with QRPA calculations performed using one of the modern phenomenological relativistic density-dependent effective interactions based on the meson-exchange representation of effective nuclear forces.

2. The quasiparticle random phase approximation

The matrix equations of the relativistic random phase approximation (RRPA) for an effective Lagrangian with explicit density dependence of the meson–nucleon couplings have been derived in Ref. [7], and for nucleon–nucleon point-coupling effective Lagrangians in Ref. [8]. The relativistic QRPA for collective excitations in open-shell nuclei has been formulated in Ref. [9] using the canonical single-nucleon basis of the relativistic Hartree–Bogoliubov (RHB) model. The extension to spin and isospin excitations (PN-QRPA) has been described in Ref. [10]. Our implementation of the PN-QRPA is identical to that of Ref. [10], with the important difference that it is now based on the point-coupling effective Lagrangian with density-dependent couplings determined by chiral pion–nucleon dynamics [1], rather than on phenomenological meson-exchange effective interactions. Here we only collect the essential expressions and refer the reader to Refs. [7–10] for technical details of the relativistic QRPA.

We consider transitions between the 0^+ ground state of a spherical even–even parent nucleus and a state with angular momentum and parity J^π of the odd–odd daughter nucleus. The spin–isospin dependent coupling terms are generated by the following interaction parts of the Lagrangian density[1]:

---

[1] Vectors in isospin space are denoted by arrows, and boldface symbols indicate vectors in ordinary three-dimensional space.

$$\mathcal{L}_{int} = \mathcal{L}_{IV} + \mathcal{L}_{\pi N} + \mathcal{L}_{LM}, \tag{1}$$

$$\mathcal{L}_{IV} = -\frac{1}{2} G_{TS}^{(\pi)}(\hat{\rho})(\bar{\psi}\vec{\tau}\psi) \cdot (\bar{\psi}\vec{\tau}\psi) - \frac{1}{2} G_{TV}^{(\pi)}(\hat{\rho})(\bar{\psi}\vec{\tau}\gamma_\mu\psi) \cdot (\bar{\psi}\vec{\tau}\gamma^\mu\psi), \tag{2}$$

$$\mathcal{L}_{\pi N} = -\frac{g_A}{2f_\pi} \bar{\psi}\gamma^\mu\gamma_5\vec{\tau}\psi \cdot \partial_\mu\vec{\phi}, \tag{3}$$

$$\mathcal{L}_{LM} = \frac{1}{2} g_0'(\hat{\rho})(\bar{\psi}\vec{\tau}\gamma_5\gamma_\mu\psi) \cdot (\bar{\psi}\vec{\tau}\gamma_5\gamma^\mu\psi). \tag{4}$$

The first term $\mathcal{L}_{IV}$ collects the isovector parts of the nuclear density functional of Ref. [1], with the density-dependent coupling strengths $G_{TS}^{(\pi)}$ and $G_{TV}^{(\pi)}$ completely determined by chiral pion–nucleon dynamics. Details are given in Ref. [1]. The same approach, without further adjustment, will also be used for the proton–neutron particle-hole (ph) residual interaction. Because of parity conservation, the one-pion direct contribution vanishes at the mean-field level in the calculation of a nuclear ground state. The pion–nucleon Lagrangian density $\mathcal{L}_{\pi N}$ Eq. (3) must be included, however, in calculations of excitations that involve spin and isospin degrees of freedom [11]. The axial vector coupling constant: $g_A = 1.3$, and the pion decay constant: $f_\pi = 92.4$ MeV.

Short-distance spin–isospin dynamics is encoded in the zero range Landau–Migdal term $\mathcal{L}_{LM}$, Eq. (4). In the non-relativistic limit the corresponding two-body interaction reduces to the familiar form $g_0'\boldsymbol{\sigma}_1 \cdot \boldsymbol{\sigma}_2\vec{\tau}_1 \cdot \vec{\tau}_2$. In a recent detailed study of the role of 2π-exchange in the interaction of quasi-nucleons at the Fermi surface $|\vec{p}_1| = |\vec{p}_2| = k_f$ [12], the four Landau–Migdal parameters $f_0(k_f)$, $f_0'(k_f)$, $g_0(k_f)$ and $g_0'(k_f)$ which characterize the four spin–isospin channels of the isotropic ($l = 0$) part of the N–N quasiparticle interaction, have been calculated using in-medium chiral perturbation theory (ChPT). This calculation includes contributions from 1π-exchange, iterated 1π-exchange and 2π-exchange with virtual $\Delta(1232)$-isobar excitations. The resulting dependence on the Fermi momentum k_f is converted into density dependence using the relation for symmetric nuclear matter: $\rho = 2k_f^3/(3\pi^2)$.

In general, the explicit density dependence of the couplings introduces additional rearrangement terms in the residual two-body interaction of the RRPA [7]. However, since these terms include the corresponding isoscalar ground-state densities, it is easy to see that they are absent in the charge-exchange channels, and the residual two-body interaction reads:

$$\begin{aligned}
V^{ph}(\boldsymbol{r}_1, \boldsymbol{r}_2) = {} & G_{TS}^{(\pi)}(\rho)\vec{\tau}_1 \cdot \vec{\tau}_2(\mathbb{1})_1(\mathbb{1})_2\delta^3(\boldsymbol{r}_1 - \boldsymbol{r}_2) \\
& + G_{TV}^{(\pi)}(\rho)\vec{\tau}_1 \cdot \vec{\tau}_2\big(\beta\gamma^\mu\big)_1(\beta\gamma_\mu)_2\delta^3(\boldsymbol{r}_1 - \boldsymbol{r}_2) \\
& + \frac{g_A^2}{16\pi f_\pi^2} \vec{\tau}_1 \cdot \vec{\tau}_2 \, (\boldsymbol{\Sigma}_1 \cdot \boldsymbol{\nabla})(\boldsymbol{\Sigma}_2 \cdot \boldsymbol{\nabla})\frac{e^{-m_\pi|\boldsymbol{r}_1 - \boldsymbol{r}_2|}}{|\boldsymbol{r}_1 - \boldsymbol{r}_2|} \\
& + g_0'(\rho)\vec{\tau}_1 \cdot \vec{\tau}_2(\beta\boldsymbol{\Sigma})_1 \cdot (\beta\boldsymbol{\Sigma})_2\delta^3(\boldsymbol{r}_1 - \boldsymbol{r}_2). \tag{5}
\end{aligned}$$

Here $\boldsymbol{\Sigma}$ is the 4×4 matrix representation of the spin operator. We note that there is no double counting of the one-pion contribution, because the Hartree diagram does not contribute to the isotropic part of the quasi-nucleon interaction in the long wavelength limit, i.e. to $g_0'(\rho)$ [12].

Pairing interactions in the particle–particle channel have also been derived using in-medium chiral dynamics [13]. However, for the convenience of quantitative comparison with previous relativistic PN-QRPA calculations for open-shell nuclei of Ref. [10], and consistent with the model that we have developed for ground-state properties in Refs. [1–3], in the $T = 1$ channel the pairing part of the Gogny force is used

$$V_{T=1}^{pp}(\mathbf{r}_1, \mathbf{r}_2) = \sum_{i=1,2} e^{-((\mathbf{r}_1 - \mathbf{r}_2)/\mu_i)^2}\big(W_i + B_i P^\sigma - H_i P^\tau - M_i P^\sigma P^\tau\big), \tag{6}$$

with the set D1S [14] for the parameters μ_i, W_i, B_i, H_i and M_i ($i = 1, 2$), and a short-range repulsive Gaussian combined with a weaker longer-range attractive Gaussian in the $T = 0$ channel:

$$V_{T=0}^{pp}(\mathbf{r}_1, \mathbf{r}_2) = -V_0 \sum_{j=1}^{2} g_j \mathrm{e}^{-((\mathbf{r}_1 - \mathbf{r}_2)/\mu_j)^2} \hat{\Pi}_{S=1,T=0}, \tag{7}$$

where $\hat{\Pi}_{S=1,T=0}$ projects onto states with $S = 1$ and $T = 0$. The ranges of the two Gaussians $\mu_1 = 1.2$ fm and $\mu_2 = 0.7$ fm are the same as for the Gogny interaction Eq. (6), and the choice of the relative strengths $g_1 = 1$ and $g_2 = -2$ makes the force repulsive at small distances. The overall strength parameter of the $T = 0$ pairing interaction $V_0 = 250$ MeV is the same as in the relativistic PN-QRPA calculation of Gamow–Teller resonances of Ref. [10]. The $T = 1$ Gogny interaction Eq. (6) is also used in the pairing channel of the RHB equations which determine the ground state of the initial nucleus. The phenomenological particle–particle interaction used here differs only slightly from the one derived from in-medium ChPT [13]. A complete investigation of in-medium pionic fluctuations (in the particle-hole and in the particle–particle channel) will be presented in a forthcoming paper.

The two-quasiparticle configuration space includes states with both nucleons in discrete bound levels, states with one nucleon in a bound level and the second nucleon in the continuum, and also states with both nucleons in the continuum. In addition to configurations built from two-quasiparticle states of positive energy, the RQRPA configuration space includes pair-configurations formed from the fully or partially occupied states of positive energy and the empty negative-energy states from the Dirac sea. In Refs. [9,10] it has been shown that the inclusion of configurations built from occupied positive-energy states and empty negative-energy states is essential for the consistency of the relativistic (proton–neutron) QRPA (current conservation, decoupling of spurious states, sum rules).

The total strength for the transition between the ground state of an even–even spherical (N, Z) nucleus and the excited state $|\lambda J\rangle$ of the corresponding odd–odd $(N + 1, Z - 1)$ or $(N - 1, Z + 1)$ nucleus, induced by an isovector single-particle operator T^{JM}, reads

$$B_{\lambda J}^{\pm} = \left| \sum_{pn} \langle p \| T^J \| n \rangle \left(X_{pn}^{\lambda J} u_p v_n + (-1)^J Y_{pn}^{\lambda J} v_p u_n \right) \right|^2, \tag{8}$$

where p and n denote proton and neutron quasiparticle canonical states, respectively, with occupation factors u_p, v_p, u_n, v_n. $X^{\lambda J}$ and $Y^{\lambda J}$ are the forward- and backward-going QRPA amplitudes for the state $|\lambda J\rangle$. The discrete strength distribution is folded with the Lorentzian function

$$R(E)^{\pm} = \frac{1}{\pi} \sum_{\lambda} B_{\lambda J}^{\pm} \frac{\Gamma/2}{(E - E_{\lambda_{\pm}})^2 + (\Gamma/2)^2}. \tag{9}$$

In the calculations performed in this work the choice for the width of the Lorentzian is 1 MeV.

2.1. Determination of $g_0'(k_f)$

The density-dependent Landau–Migdal parameter $g_0'(k_f)$ of Ref. [12] can be expanded in powers of the Fermi momentum k_f to the same order as $G_{TS}^{(\pi)}(k_f)$ and $G_{TV}^{(\pi)}(k_f)$ [1]:

$$g_0'(k_f) = c_1 + c_2 \frac{k_f}{\Lambda} + c_3 \left(\frac{k_f}{\Lambda} \right)^2 + c_4 \left(\frac{k_f}{\Lambda} \right)^3, \tag{10}$$

Table 1

Coefficients in the expansion of the spin–isospin Landau–Migdal parameter $g'_0(k_f)$ Eq. (10). The best-fit constants used in the present calculation (middle column), are shown in comparison with the estimates of Refs. [6,12] (right column)

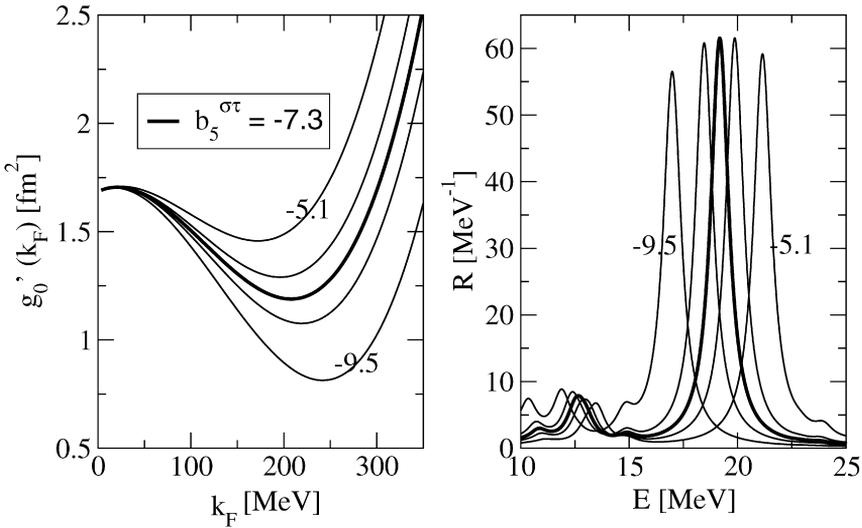| Coefficients		Constants	
c_1 (fm^2)	-1.80 fm$^2 - \frac{\pi^2}{\Lambda^2} b_3$	$b_3 = -2.93$	-3.05 [6]
c_2 (fm^2)	1.17 fm^2		
c_3 (fm^2)	-9.84 fm$^2 + \frac{\pi^2}{\Lambda^2} b_5^{\sigma\tau}$	$b_5^{\sigma\tau} = -7.30$	-8.03 [12]
c_4 (fm^2)	21.13 fm$^2 - \frac{\pi^2}{\Lambda^2} b_6^{\sigma\tau}$	$b_6^{\sigma\tau} = -8.45$	-8.45 [12]

Fig. 1. Left panel: the Landau–Migdal parameter g'_0 as function of the Fermi momentum k_f for several values of $b_5^{\sigma\tau}$ in the interval $[-5.1, -9.5]$. In the panel on the right the corresponding Gamow–Teller strength functions in ^{208}Pb are shown. The experimental position of the GTR is reproduced with the choice: $b_5^{\sigma\tau} = -7.30$.

with the coefficients c_i listed in Table 1, and $\Lambda = 2\pi f_\pi \simeq 0.58$ GeV chosen as a reference scale. We note that, in addition to the terms which are completely determined by the in-medium ChPT calculation of pion-exchange diagrams, the constants c_1, c_3 and c_4 involve three parameters as displayed in Table 1: b_3, $b_5^{\sigma\tau}$ and $b_6^{\sigma\tau}$, respectively, which encode the additional short-range dynamics of the NN and $3N$ interactions. In Ref. [6] the subtraction constant $b_3 = -3.05$ was adjusted to empirical nuclear matter properties at saturation point. Taking into account ground-state properties of finite nuclei in addition, this constant has been fine-tuned to $b_3 = -2.93$ in Ref. [1]. This latter value will consistently be used both in the Dirac Hamiltonian which determines the nuclear ground state, and in the isovector residual RPA interaction Eq. (5). The remaining two short-distance constants $b_5^{\sigma\tau}$ and $b_6^{\sigma\tau}$ cannot be constrained by ground-state properties of spin-saturated nuclear matter. In Ref. [12] the value of $b_5^{\sigma\tau}$ has been adjusted so that the resulting g'_0 is consistent with empirical values at saturation density. Here we retain the value $b_6^{\sigma\tau} = -8.45$ from Ref. [12], and adjust $b_5^{\sigma\tau}$ in such a way that the PN-RPA calculation reproduces the excitation energy of the Gamow–Teller giant resonance (GTR) in ^{208}Pb. In Fig. 1 we plot the Landau–Migdal parameter g'_0 as a function of the Fermi momentum k_f for several
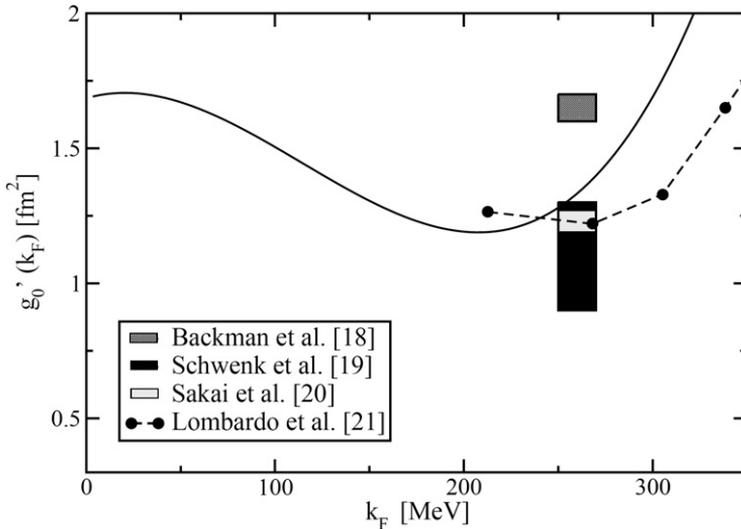
Fig. 2. The dimensionfull Landau–Migdal parameter g'_0 as function of the Fermi momentum k_f (solid curve). The values around saturation point are compared with those reported in Refs. [18] (dark gray rectangle), [19] (black rectangle), and [20] (light gray rectangle). The black dots are the values obtained with the Brueckner–Hartree–Fock calculation of Ref. [21]. The dimensionless G'_0 values from Refs. [18–21] have been divided by the density of states at the Fermi surface $N_0 = 2\pi^{-2} k_{f0} M^* \approx 1$ fm^{-2}.

values of $b_5^{\sigma\tau}$ in the interval $[-5.1, -9.5]$. In the panel on the right the corresponding Gamow–Teller strength functions in ^{208}Pb. The experimental position of the GTR in ^{208}Pb: 19.2 MeV [15–17], is reproduced with $b_5^{\sigma\tau} = -7.30$. This value is remarkably close to the estimate of Ref. [12].

With the constants b_3, $b_5^{\sigma\tau}$ and $b_6^{\sigma\tau}$ adjusted as described above, we plot the resulting g'_0 as a function of the Fermi momentum in Fig. 2. The values around saturation point ($k_f \approx 260$ MeV) are compared with: (a) a Brueckner calculation with a phenomenological NN-interaction [18] (dark gray rectangle); (b) a recent estimate based on the universal low-momentum potential $V_{low\text{-}k}$ [19] (black rectangle); (c) an empirical estimate based on the quenching of the Gamow–Teller strength [20] (light gray rectangle). We notice good agreement between the predicted values of g'_0 at saturation density, even though they have been obtained with very different models or estimated empirically. The functional dependence for $k_f > 200$ MeV is in qualitative agreement with the Brueckner–Hartree–Fock calculation of Ref. [21] (black dots), which has employed the Argonne V_{18} two-body potential [22], and a three-body force from Ref. [23].

3. Applications: Spin–isospin collective excitations

Collective spin and isospin excitations in nuclei have been the subject of numerous experimental and theoretical studies (for extensive reviews see Refs. [24,25]). Nucleons with spin up and spin down can oscillate either in phase (spin scalar $S = 0$ mode) or out of phase (spin vector $S = 1$ mode). The spin vector, or spin-flip excitations can be of isoscalar ($S = 1$, $T = 0$) or isovector ($S = 1$, $T = 1$) nature. These modes provide information on the spin and spin–isospin channels of effective nuclear interactions.
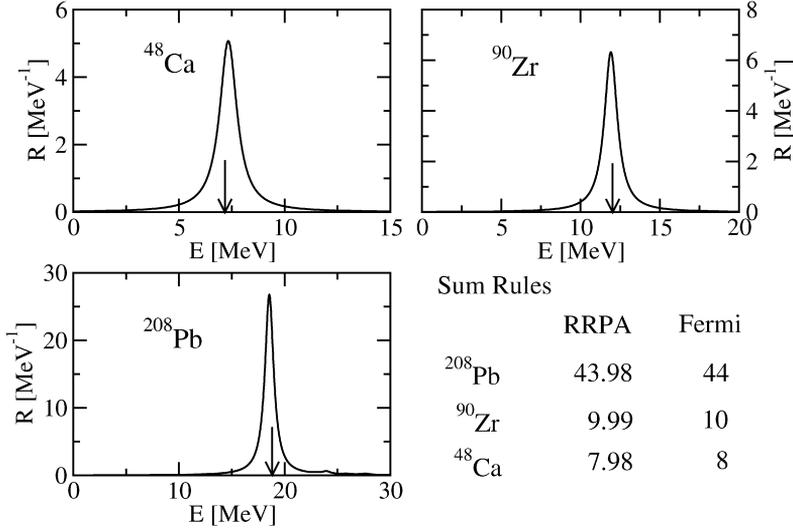
Fig. 3. PN-RRPA $J^\pi = 0^+$ strength distributions. The excitations of the isobaric analog resonances are compared with experimental data (arrows) for ^{48}Ca [26], ^{90}Zr [27], and ^{208}Pb [15,28]. The integrated strengths are compared to the model-independent Fermi sum rule Eq. (12).

3.1. Isobaric analog resonances

As a first application of this new PN-QRPA model, we calculate the strength functions for the simplest charge–exchange mode: the isobaric analog resonance (IAR) $J^\pi = 0^+$. The one-body Fermi transition operator reads:

$$T^F_{\beta\mp} = \sum_{i=1}^{A} \tau_\mp(i). \tag{11}$$

For $N > Z$ nuclei $T^F_{\beta-}$ simply changes a neutron into a proton without spin-flip or change in orbital angular momentum. In Fig. 3 we plot the calculated PN-QRPA response to the operator Eq. (11) for ^{48}Ca, ^{90}Zr and ^{208}Pb. The strength distributions are dominated by a single IAR peak which corresponds to a coherent superposition of proton-particle–neutron-hole excitations. The calculated IAR excitation energies (evaluated with respect to the calculated ground state of the parent nucleus) are compared with the corresponding experimental values from (p, n) charge-exchange scattering data for ^{48}Ca (7.2 MeV) [26], ^{90}Zr (12.0 MeV) [27], and ^{208}Pb (18.8 MeV) [28]. The agreement between the PN-QRPA results and experimental data is very good. We have also verified that the calculated strength distributions exhaust the Fermi sum rule

$$S^F_{\beta-} = \sum_f \left| \langle \psi_f | T^F_{\beta-} | \psi_i \rangle \right|^2 = 2\langle \psi_i | T_3 | \psi_i \rangle = N - Z, \tag{12}$$

to better than 99.75% (see Fig. 3).

As a second example we consider open-shell nuclei and plot, in Fig. 4, the calculated IAR excitation energies for the sequence of even–even Sn target nuclei with $A = 108$–132. The result of our self-consistent RHB plus PN-QRPA calculation are shown in comparison with experimental data obtained in a systematic study of the $(^3\text{He, t})$ charge-exchange reaction over the entire
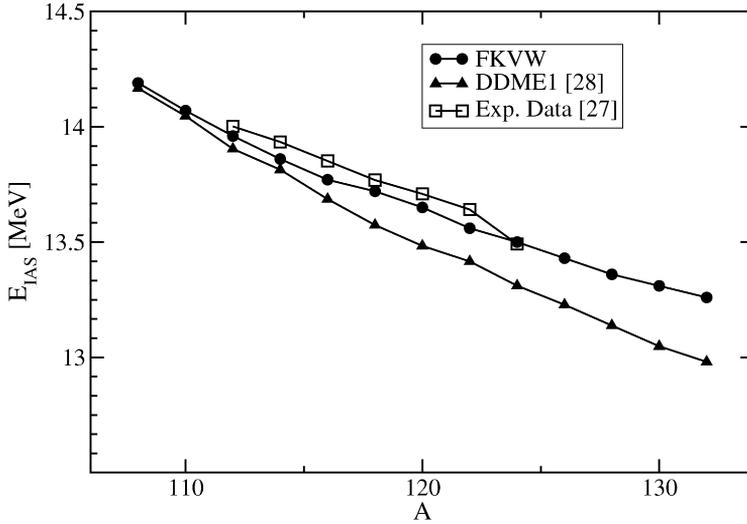
Fig. 4. RHB plus PN-QRPA results for the isobaric analog resonances of the sequence of even–even Sn target nuclei, calculated with the FKVW + Gogny effective interaction and compared with experimental data [32], and with the calculation of Ref. [10].

range of stable Sn isotopes [32], and with the relativistic PN-QRPA analysis of Ref. [10], in which the phenomenological density-dependent meson-exchange interaction DD-ME1 [33] was used both in the RHB calculation of the ground states and in the particle-hole (*ph*) channel of the isovector residual interaction. Both models reproduce the empirical mass dependence of the IAR, and the calculated excitation energies are in very good agreement with available data. For DD-ME1 the largest difference between the theoretical and experimental IAR excitation energies is ≈ 200 keV, and an even better agreement with data is obtained in the present calculation. This is because the FKVW effective interaction reproduces the ground states of Sn isotopes (e.g. binding energies) better than DD-ME1 [1]. We note that, because the IAR is a non-spin-flip mode, the one-pion exchange Eq. (3) and the Landau–Migdal term Eq. (4) do not contribute to the matrix elements of the residual interaction Eq. (5). The only contribution comes from the isovector channel of the FKVW interaction (i.e. the Lagrangian density Eq. (2)). The density-dependent coupling strengths $G_{TS}^{(\pi)}$ and $G_{TV}^{(\pi)}$ have been adjusted to the (asymmetric) nuclear matter equation of state and ground-state properties of finite nuclei.

We would also like to emphasize a result that was already discussed in Ref. [10], namely that sharp, non-fragmented IAR peaks in open-shell nuclei are only obtained when the $T = 1$ pairing interaction is consistently included both in the RHB calculation of the nuclear ground-state and in the proton–neutron residual interaction. This is simply a consequence of the fact that the pairing interaction is isospin invariant, and therefore commutes with the Fermi operator Eq. (11).

We note that the Nolen–Schiffer anomaly [29] is absent in the present calculation because the attractive Coulomb exchange term is not included in the energy density functional that we use in the calculation of ground state properties [30]. Further refinements should also consider charge symmetry breaking contributions, e.g. from iterated and irreducible pion–photon exchange processes [31].
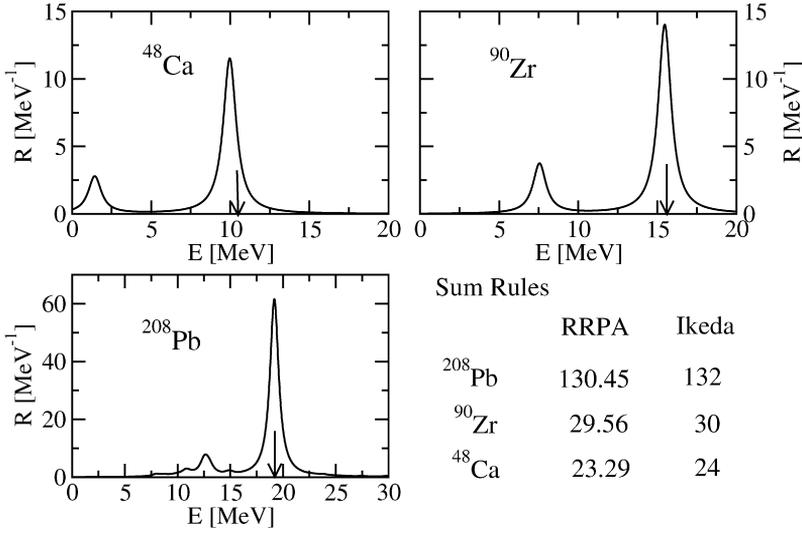
Fig. 5. Gamow–Teller strength distributions for ^{48}Ca, ^{90}Zr and ^{208}Pb. PN-RQPA results are shown in comparison with experimental data (arrows) for the GTR excitation energies in ^{48}Ca [26], ^{90}Zr [27,28], and ^{208}Pb [15–17].

3.2. Gamow–Teller excitations

The calculated Gamow–Teller ($J^\pi = 1^+$) strength distributions for ^{48}Ca, ^{90}Zr and ^{208}Pb are shown in Fig. 5. The one-body Gamow–Teller operator reads:

$$T_{\beta\mp}^{GT} = \sum_{i=1}^{A} \Sigma(i)\tau_\mp(i). \tag{13}$$

The corresponding integrated strengths satisfy the Ikeda sum rule:

$$S_{\beta-}^{GT} - S_{\beta+}^{GT} = \sum_f |\langle\psi_f|T_{\beta-}^{GT}|\psi_i\rangle|^2 - \sum_f |\langle\psi_f|T_{\beta+}^{GT}|\psi_i\rangle|^2 = 3(N-Z). \tag{14}$$

In addition to the high-energy GT resonance—a collective superposition of direct spin-flip ($j = l + \frac{1}{2} \to j = l - \frac{1}{2}$) transitions—the response functions display a concentration of strength in the low-energy tail. The transitions in the low-energy region correspond to core-polarization ($j = l \pm \frac{1}{2} \to j = l \pm \frac{1}{2}$), and back spin-flip ($j = l - \frac{1}{2} \to j = l + \frac{1}{2}$) neutron-hole–proton-particle excitations. The calculated GTR are compared with the experimental excitation energies: 10.5 MeV for ^{48}Ca [26], 15.6 MeV for ^{90}Zr [27,28], and 19.2 MeV for ^{208}Pb [15–17]. Although one of the parameters of the Landau–Migdal interaction has been adjusted to reproduce the GTR excitation energy in ^{208}Pb, we find a very good agreement with experiment also for ^{48}Ca and ^{90}Zr. The integrated strengths satisfy the Ikeda sum rule with high accuracy. This is an important test of the internal consistency of our relativistic PN-RPA. We note that the Ikeda sum rule is exhausted by the calculated GT strength only when the relativistic RPA/QRPA space includes both the *ph* excitations formed from ground-state configurations of the fully or partially occupied states of positive energy, and the empty negative-energy states from the Dirac sea [10]. The contribution of these configurations to the Ikeda sum rule is of the order of 8–10%.

Finally, for the sequence of even–even Sn target nuclei, we compare in Fig. 6 the PN-QRPA predictions for the GTR excitation energies with experimental data from Sn(^{3}He, t)Sb charge-
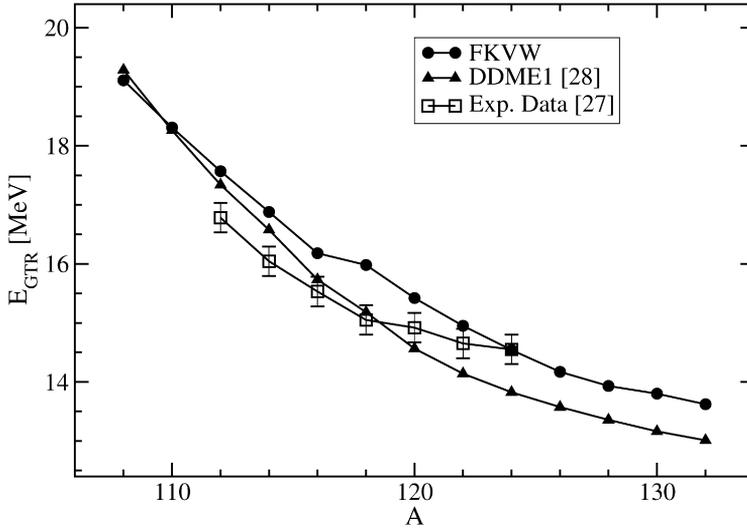
Fig. 6. Excitation energies of Gamow–Teller resonances for the sequence of even–even $^{108-132}$Sn target nuclei. The present relativistic PN-QRPA calculation is compared with the results of Ref. [10], and with experimental data from Ref. [32].

exchange reactions [32], and with the results obtained with the DD-ME1 meson-exchange effective interaction in Ref. [10]. The same $T = 1$ Eq. (6) and $T = 0$ Eq. (7) pairing interactions have been used in both PN-QRPA calculations. Both models reproduce the isotopic trend of GTR excitation energies. For the individual nuclei the level of agreement with data varies. Below $A = 120$ the GTR calculated with DD-ME1 plus the residual interaction of Ref. [10] are closer to the experimental energies, whereas for $A > 120$ the present PN-QRPA calculation using the FKVW parameterization plus the residual interaction Eq. (5) predicts GTR in better agreement with data.

4. Conclusions

In summary, we have extended our approach to nuclear density functional theory, based on chiral dynamics and the symmetry breaking pattern of low-energy QCD, to the description of charge-exchange excitations in finite nuclei. Starting from the relativistic nuclear density functional (FKVW) introduced in Ref. [1], the proton–neutron (quasiparticle) random phase approximation has been formulated and applied in a study of the role of chiral pion–nucleon dynamics in excitation modes which include spin and isospin degrees of freedom. In addition to the isovector channel of the FKVW effective interaction, the RPA residual interaction includes the direct one-pion exchange and the zero-range Landau–Migdal term.

The density dependence of the Landau–Migdal parameter $g'_0(k_f)$ which characterizes the spin–isospin channel of the isotropic part of the quasi-nucleon interaction at the Fermi surface, has been calculated in Ref. [12] using in-medium ChPT. In the present work one of the short-distance constants has been fine-tuned in such a way that the relativistic PN-QRPA calculation reproduces the excitation energy of the Gamow–Teller resonance (GTR) in ^{208}Pb. Both approaches lead to very similar values of $g'_0(k_f)$. In addition to the residual interaction in the ph channel, the model includes both the $T = 1$ and $T = 0$ pairing channels. PN-QRPA calculations have been performed for the $J^\pi = 0^+$ and $J^\pi = 1^+$ charge exchange modes in ^{48}Ca, ^{90}Zr

and ^{208}Pb, and for a sequence of even–even $^{108-132}$Sn nuclei. Results for the excitation energies of IAR and GTR, and especially for the isotopic trend in the chain Sn nuclei, are in very good agreement with available data and with calculations performed using modern phenomenological relativistic density-dependent meson-exchange effective interactions.

This analysis has shown that a nuclear energy density functional based on chiral effective field theory provides a consistent microscopic framework not only for ground-state properties, but also for complex excitations of the nuclear many-body system. The specific density dependence of spin–isospin dependent particle-hole interactions, as derived from in-medium chiral dynamics, gives a successful description of both isobaric analogue and Gamow–Teller modes.

Acknowledgements

References

[1] P. Finelli, N. Kaiser, D. Vretenar, W. Weise, Nucl. Phys. A 770 (2006) 1.
[2] P. Finelli, N. Kaiser, D. Vretenar, W. Weise, Eur. Phys. J. A 17 (2003) 573.
[3] P. Finelli, N. Kaiser, D. Vretenar, W. Weise, Nucl. Phys. A 735 (2004) 449.
[4] D. Vretenar, W. Weise, in: G. Lalazissis, P. Ring, D. Vretenar (Eds.), Lecture Notes in Physics, vol. 641, Springer-Verlag, Heidelberg, 2004, p. 61.
[5] N. Kaiser, T. Nikšić, D. Vretenar, Eur. Phys. J. A 25 (2005) 257.
[6] S. Fritsch, N. Kaiser, W. Weise, Nucl. Phys. A 750 (2005) 259.
[7] T. Nikšić, D. Vretenar, P. Ring, Phys. Rev. C 66 (2002) 064302.
[8] T. Nikšić, D. Vretenar, P. Ring, Phys. Rev. C 72 (2005) 014312.
[9] N. Paar, P. Ring, T. Nikšić, D. Vretenar, Phys. Rev. C 67 (2003) 034312.
[10] N. Paar, T. Nikšić, D. Vretenar, P. Ring, Phys. Rev. C 69 (2004) 054303.
[11] T.E.O. Ericson, W. Weise, Pions and Nuclei, Oxford Univ. Press, 1988.
[12] N. Kaiser, Nucl. Phys. A 768 (2006) 99.
[13] N. Kaiser, T. Nikšić, D. Vretenar, Eur. Phys. J. A 25 (2005) 257.
[14] J.F. Berger, M. Girod, D. Gogny, Comput. Phys. Commun. 63 (1991) 365.
[15] H. Akimune, et al., Phys. Rev. C 52 (1995) 604.
[16] D.J. Horen, et al., Phys. Lett. B 95 (1980) 27.
[17] A. Krasznahorkay, et al., Phys. Rev. C 64 (2001) 067302.
[18] S.O. Bäckman, G.E. Brown, J.A. Niskanen, Phys. Rep. 124 (1985) 1.
[19] A. Schwenk, G.E. Brown, B. Friman, Nucl. Phys. A 703 (2002) 745.
[20] H. Sakai, Nucl. Phys. A 731 (2004) 94.
[21] W. Zuo, C. Shen, U. Lombardo, Phys. Rev. C 67 (2003) 037301.
[22] R.B. Wiringa, V.G.J. Stoks, R. Schiavilla, Phys. Rev. C 51 (1995) 38.
[23] P. Grange, A. Lejeune, M. Martzoff, J.-F. Mathiot, Phys. Rev. C 40 (1989) 1040.
[24] F. Osterfeld, Rev. Mod. Phys. 64 (1992) 491.
[25] M.N. Harakeh, A.M. Van Der Woude, Giant Resonances: Fundamental High-Frequency Modes of Nuclear Excitations, Oxford Univ. Press, 2001.
[26] B.D. Anderson, et al., Phys. Rev. C 31 (1985) 1161.
[27] T. Wakasa, et al., Phys. Rev. C 55 (1997) 2909.
[28] D.E. Bainum, Phys. Rev. Lett. 44 (1980) 1751.
[29] J.A. Nolen, J.P. Schiffer, Annu. Rev. Nucl. Sci. 19 (1969) 471.
[30] B.A. Brown, W.A. Richter, R. Lindsay, Phys. Lett. B 483 (2000) 49.
[31] N. Kaiser, Phys. Rev. C 69 (2004) 034337.
[32] K. Pham, et al., Phys. Rev. C 51 (1995) 526.
[33] T. Nikšić, D. Vretenar, P. Finelli, P. Ring, Phys. Rev. C 66 (2002) 024306.